

Beam Geometry Calibration of Sodars without Use of a Mast

STUART BRADLEY

Physics Department, University of Auckland, Auckland, New Zealand

SABINE VON HÜNERBEIN

Acoustics Research Centre, University of Salford, Salford, United Kingdom

(Manuscript received 21 May 2012, in final form 29 January 2013)

ABSTRACT

A new method for calibration of sodar wind speed measurements is described. The method makes no assumptions whatsoever about the sodar operation and its hardware and software, other than the assumption that only one beam is transmitted at a time. Regardless of the complexity of the actual beam shape, the *effective* beam zenith angle is accurately estimated: this is the angle that must be used in estimations of velocity components. In a very simple experiment, the effective beam zenith angle has been found to within around 0.2° , which is as good as is required in the most stringent sodar calibration procedures. It has been found, even for such a short data run, that the estimated beam angle is very close to that calculated from the sodar array geometry. The main limitation is the requirement for horizontally homogeneous flow, since the regression methods use both a tilted beam and a vertical beam. Note that this is also a fundamental limiting assumption in the normal operation of ground-based wind lidars and sodars.

1. Introduction

Sodars transmit a short pulse in at least three upward directions. Scattering from atmospheric turbulent refractive index fluctuations results in a time series signal from each direction. Spectral analysis of time-gated segments of these time series gives a spectral peak whose frequency is a measure of the Doppler shift from the moving scatterers. Using at least three independent acoustic beams assures a system of at least three equations in the vector wind Cartesian components $\mathbf{V} = (u, v, w)$. Solving this set of equations then gives a wind profile with estimates at the center of each height represented by the center of each time gate (Bradley 2008).

There is very little that can “go wrong” with such a design. Nevertheless, large efforts have been expended on comparisons between mast-mounted anemometers and sodars in such experiments as the Profiler Intercomparison Experiment (PIE; Bradley et al. 2005), directed toward remote sensing becoming a viable replacement for mast instrumentation. The most important findings of PIE were that a sodar gives similar variability in wind speeds

to a cup anemometer, but there remain small systematic errors in wind speeds estimated by a sodar. Such biases can be detected through sodar–mast comparisons, but these are, in general, rather inconvenient. Therefore, we consider a new method for doing in situ field calibrations of wind measurements from a sodar. This method has huge advantages of requiring neither a comparison against some other “standard” nor any assumptions regarding sodar geometry and operation.

The method is equally applicable to wind lidars. However, the emphasis on sodars is warranted because it is difficult to test a full-size sodar system in an anechoic facility. Also, the acoustic beam from a sodar has greater width than the optical beam from a lidar, and therefore the equivalent volume-averaged Doppler shift is likely to be less well known. This is rather difficult to estimate a priori, as opposed to the beam azimuth angle or the central pointing direction of a vertical beam, which are well determined by the sodar antenna geometry.

2. Sodar wind measurement calibration

a. Traditional calibration

Monostatic sodars use beams tilted from the vertical. The signal scattered back to the receiver in each tilted beam is Doppler shifted according to the radial component

Corresponding author address: Stuart Bradley, Physics Department, University of Auckland, Private Bag 92019, Auckland, New Zealand.
E-mail: s.bradley@auckland.ac.nz

V_r of wind velocity \mathbf{V} in the beam direction. For a thin beam in direction $\mathbf{\Omega}_0 = (\cos\phi_0 \sin\theta_0, \sin\phi_0 \sin\theta_0, \cos\theta_0)$ and wind velocity $\mathbf{V} = (u, v, w)$,

$$V_r = \mathbf{V} \cdot \mathbf{\Omega}_0 = u \cos\phi_0 \sin\theta_0 + v \sin\phi_0 \sin\theta_0 + w \cos\theta_0. \quad (1)$$

At least three independent measurements are needed to solve for (u, v, w) . We will concentrate on the typical three-beam design. The system of equations

$$\mathbf{R} = \mathbf{B}\mathbf{V}$$

is solved, where \mathbf{R} is the 3×1 vector of measured radial velocity components, \mathbf{B} is the 3×3 weighting matrix, and \mathbf{V} is the 3×1 vector of unknown wind velocity components. The solution $\hat{\mathbf{V}} = \mathbf{B}^{-1}\mathbf{R}$ is used to form $(\hat{u}^2 + \hat{v}^2 + \hat{w}^2)^{1/2} = (\hat{\mathbf{V}} \cdot \hat{\mathbf{V}})^{1/2}$ for comparison with $(u^2 + v^2 + w^2)^{1/2} = (\mathbf{V} \cdot \mathbf{V})^{1/2}$ measured by a mast-mounted anemometer. By this method a *single* calibration parameter

$$m = (\hat{\mathbf{V}} \cdot \hat{\mathbf{V}})^{1/2} / (\mathbf{V} \cdot \mathbf{V})^{1/2} \quad (2)$$

is obtained.

$$m^2 = \left(\frac{\hat{V}}{V} \right)^2 = \frac{\sin^2\theta_0}{\sin^2\hat{\theta}} + \frac{w(\cos\theta_0 - \cos\hat{\theta})[2(u+v)\sin\theta_0 + w(2 + \cos\theta_0 + \cos\hat{\theta})]}{(u^2 + v^2 + w^2)\sin^2\hat{\theta}},$$

where $\hat{\theta}$ is the tilt angle assumed by the software and θ_0 is the actual tilt angle. This problem with traditional calibration methods has not been previously considered.

In practice, however, the beam is not an angular delta function and the weights in (1) are volume averages over the transmitted and received beams,

$$V_r = \overline{u \cos\phi \sin\theta} + \overline{v \sin\phi \sin\theta} + \overline{w \cos\theta}. \quad (3)$$

The elements of \mathbf{B} could be found in principle by measuring the beam angular intensity variations in an anechoic chamber, or perhaps in the field, but this effort would be large because of the need to capture beam details on a hemispherical surface in high angular resolution in 2D, so that the proper volume averages can be calculated.

3. Tilt angle perturbation

a. Basic perturbation concept

Figure 1 shows the x - z plane for a sodar having a beam at an initial effective tilt angle θ_1 . If there is also a beam in the y - z plane tilted at an angle of θ_2 to the vertical, then the equations corresponding to (1) are

Consider the following simple example: A very narrow beam in the x - z plane and with $w = 0$ has $V_r = u \sin\theta_0$, so the wind estimate is $\hat{u} = V_r / \sin\theta_0$. If there is an uncertainty or an error $\Delta\theta$ in the tilt angle θ_0 , then the uncertainty or error in estimated wind is $\Delta\hat{u}/\hat{u} = -\Delta\theta/\tan\theta_0$. For $\theta_0 = 15^\circ$, each 1° error in beam pointing angle gives a 5% error in the estimation of wind speed: monostatic sodars and lidars are highly sensitive to beam pointing.

b. Complete wind measurement calibration

The calibration parameter m in (2) contains combinations of elements from beam matrix \mathbf{B} , which are functions of the three zenith angles and three azimuth angles for a three-beam system. In obtaining estimates of u, v , and w , these elements are assumed known in the sodar processing software. Incorrect values of any of these elements will give a variation in m . This variation in m will also be wind-direction dependent, as can be seen from the very simple case of a beam tilted an angle θ_0 in the x - z plane, another beam tilted θ_0 in the y - z plane, and the third beam vertical. Then,

$$V_{r1} = u \sin\theta_1 + w \cos\theta_1, \quad (4)$$

$$V_{r2} = v \sin\theta_2 + w \cos\theta_2, \quad \text{and} \quad (5)$$

$$V_{r3} = w. \quad (6)$$

Also shown is the entire sodar rotated by an angle $\Delta\theta$ about the y axis. Now,

$$V_{r1}^* = u \sin(\theta_1 + \Delta\theta) + w \cos(\theta_1 + \Delta\theta), \quad (7)$$

$$V_{r2}^* = u \sin(\Delta\theta) \cos\theta_2 + v \sin\theta_2 + w \cos(\Delta\theta) \cos\theta_2, \quad \text{and} \quad (8)$$

$$V_{r3}^* = u \sin(\Delta\theta) + w \cos(\Delta\theta). \quad (9)$$

The V_{r1}, V_{r3}, V_{r1}^* , and V_{r3}^* quantities are measured; the tilt perturbation $\Delta\theta$ is known; and u, w, θ_1 , and θ_2 are unknown. Equations (4)–(9) are nonlinear in the unknowns, but they can be solved by finding w using (6), u using (9), $\sin\theta_1$ using (4) and (7), $\cos\theta_2$ using (5) and (8), and v using (5), giving

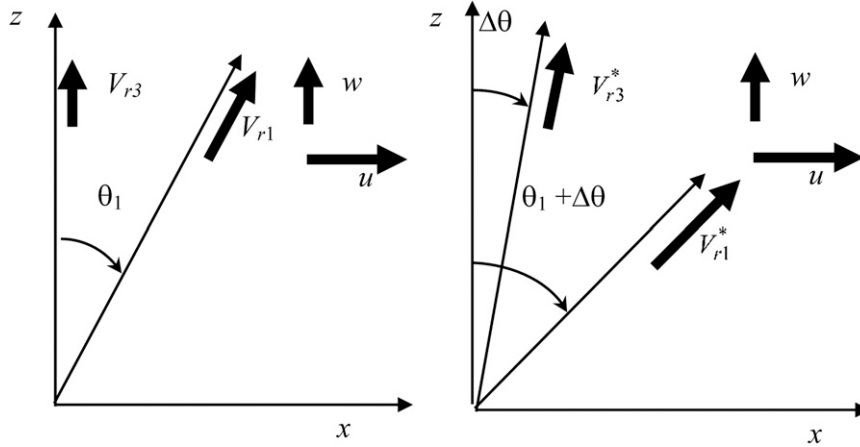


FIG. 1. (left) Geometry of a sodar beam tilted at an angle θ_1 and (left) with the sodar rotated by an angle $\Delta\theta$ about the y axis. Wind velocity components in this plane are u and w , and the along-beam radial components for the two beams in this plane are V_{r1} and V_{r3} .

$$u = \frac{V_{r3}^* - V_{r3} \cos\Delta\theta}{\sin\Delta\theta}, \tag{10}$$

$$\cos\theta_2 = \frac{V_{r2}^* - V_{r2}}{V_{r3}^* - V_{r3}}. \tag{14}$$

$$v = \frac{(V_{r2} V_{r3}^* - V_{r3} V_{r2}^*)(V_{r3}^* - V_{r3})}{\sqrt{(V_{r3}^* - V_{r3})^2 - (V_{r2}^* - V_{r2})^2}}, \tag{11}$$

b. The effective tilt angle

$$w = V_{r3}, \tag{12}$$

As indicated in (3), components of \mathbf{B} are volume averages. The volume averaging means that a normalized beam gain function $G(\mathbf{\Omega}, \mathbf{\Omega}_0)$ is averaged over solid angle $\mathbf{\Omega}$ around a pointing direction $\mathbf{\Omega}_0$ in each of the terms on the right of (1):

$$\sin\theta_1 = \frac{V_{r1} V_{r3}^* - V_{r1}^* V_{r3}}{V_{r3}^2 - 2V_{r3} V_{r3}^* \cos\Delta\theta + V_{r3}^{*2}} \sin\Delta\theta, \text{ and} \tag{13}$$

$$\begin{aligned} V_r &= \int_{\Omega} \mathbf{\Omega} \cdot \mathbf{V} G(\mathbf{\Omega}, \mathbf{\Omega}_0) d\Omega = \int_{\Omega} (u \cos\phi \sin\theta + v \sin\phi \sin\theta + w \cos\theta) G(\mathbf{\Omega}, \mathbf{\Omega}_0) d\Omega \\ &= u \int_{\Omega} \cos\phi \sin\theta G(\mathbf{\Omega}, \mathbf{\Omega}_0) d\Omega + v \int_{\Omega} \sin\phi \sin\theta G(\mathbf{\Omega}, \mathbf{\Omega}_0) d\Omega + w \int_{\Omega} \cos\theta G(\mathbf{\Omega}, \mathbf{\Omega}_0) d\Omega \\ &= \overline{u \cos\phi \sin\theta} + \overline{v \sin\phi \sin\theta} + \overline{w \cos\theta}, \end{aligned} \tag{15}$$

where

This means that

$$\iint_{\Omega} G(\mathbf{\Omega}, \mathbf{\Omega}_0) d\Omega = 1.$$

$$V_r = \overline{u \cos\phi \sin\theta} + \overline{w \cos\theta} = u \sin\theta_1 + w \cos\theta_1.$$

For a beam nominally in the x - z plane, there will be contributions from finite azimuth angles ϕ . However, such beams are invariably symmetric in azimuth, so G is an even function of ϕ and the integral

The θ_1 appearing in (4) is therefore an *effective* beam tilt angle. If this is perturbed by rotating the entire sodar through $\Delta\theta$ about the y axis, then, using an angular coordinate system attached to the sodar, $G(\mathbf{\Omega}, \mathbf{\Omega}_0)$ remains unchanged but the beam direction with respect to the wind \mathbf{V} is now $[\cos\phi \sin(\theta + \Delta\theta), \sin\phi \sin(\theta + \Delta\theta), \cos(\theta + \Delta\theta)]$. The first term on the right of (15) becomes

$$\int_{\Omega} \sin\phi \sin\theta G(\mathbf{\Omega}, \mathbf{\Omega}_0) d\Omega = 0.$$

$$\begin{aligned}
 u \int_{\Omega} \cos\phi \sin(\theta + \Delta\theta) G(\mathbf{\Omega}, \mathbf{\Omega}_0) d\Omega &= u \int_{\Omega} \cos\phi (\sin\theta \cos\Delta\theta + \cos\theta \sin\Delta\theta) G(\mathbf{\Omega}, \mathbf{\Omega}_0) d\Omega \\
 &= u \cos\Delta\theta \int_{\Omega} \cos\phi \sin\theta G(\mathbf{\Omega}, \mathbf{\Omega}_0) d\Omega + u \sin\Delta\theta \int_{\Omega} \cos\phi \cos\theta G(\mathbf{\Omega}, \mathbf{\Omega}_0) d\Omega \\
 &= u \cos\Delta\theta \overline{\cos\phi \sin\theta} + u \sin\Delta\theta \overline{\cos\phi \cos\theta} = u \cos\Delta\theta \sin\theta_1 + u \sin\Delta\theta \cos\theta_1 \\
 &= u \sin(\theta_1 + \Delta\theta).
 \end{aligned}$$

This means that, although θ_1 is an effective zenith angle and not necessarily the same as the pointing zenith angle, we can validly do arithmetic such as $\sin(\theta_1 + \Delta\theta) = \sin\theta_1 \cos(\Delta\theta) + \sin(\Delta\theta) \cos\theta_1$ as in (4)–(14).

4. The effect of beam geometry on Doppler shift

In the above, the Doppler shift is contained in the elements of vector \mathbf{R} . The weighting on each of the wind velocity components is volume averaged, but this does not give any indication of the spread or shape of the Doppler spectrum from which, by detecting the peak position, the components of \mathbf{R} are estimated.

The acoustic radar equation covers this in principle (Bradley 2008). Including the dependence on frequency and on volume averaging, the spectral density of received power at the monostatic antenna equation becomes

$$\frac{dP_R}{df} = c\tau\sigma_s \frac{e^{-2\alpha r}}{r^2} \int_{\Omega} \frac{dP_T}{df} G(\mathbf{\Omega}) d\Omega.$$

$$\int_0^{2\pi} \left(\int_{-\pi/2}^{\pi/2} \exp \left\{ -\frac{1}{2\sigma_f^2} \left[f - f_T \left(1 - 2\frac{u}{c} \sin\theta \cos\phi - 2\frac{v}{c} \sin\theta \sin\phi - 2\frac{w}{c} \cos\theta \right) \right]^2 \right\} G \sin\theta d\theta \right) d\phi. \quad (16)$$

The usual assumption is that the beam in the x - z plane is effectively an angular delta function,

$$G(\theta, \phi) = \cos\theta \delta(\theta - \theta_0) \delta(\phi).$$

Then, the above integral becomes

$$\exp \left\{ -\frac{1}{2\sigma_f^2} \left[f - f_T \left(1 - 2\frac{u}{c} \sin\theta_0 - 2\frac{w}{c} \cos\theta_0 \right) \right]^2 \right\} \sin\theta_0 \cos\theta_0,$$

so that the spectrum peaks at

$$f_x = f_T \left(1 - 2\frac{u}{c} \sin\theta_0 - 2\frac{w}{c} \cos\theta_0 \right),$$

Here, c is the speed of sound, τ is the pulse duration, σ_s is the scattering cross-section area per unit volume and per unit solid angle, α is the acoustic absorption, r is the range to the scattering volume, dP_T/df is the power-per-unit frequency interval transmitted into solid angle $d\Omega$, and G is an angle-dependent sensitivity kernel. The atmospheric absorption and scattering parts have been taken outside of the scattering volume integral since they are only weakly frequency dependent, and it is assumed that they do not vary much within a typical scattering volume. Assuming a Gaussian-shaped transmitted pulse of spectral width σ_f and that the Doppler spectrum is centered on f_D rather than transmitted frequency f_T ,

$$\frac{dP_R}{df} \propto \int_{\Omega} \exp \left[-\frac{1}{2\sigma_f^2} (f - f_D)^2 \right] G(\mathbf{\Omega}) d\Omega.$$

Note that all commercial sodars use an approximately Gaussian pulse shape.

For example, if the acoustic beam has sensitivity G at a zenith angle θ and azimuth angle ϕ , then the integral is

giving the expected radial component as in (1) with $\phi_0 = 0$. Similarly, it is usually assumed that the beam in the $+z$ direction has the form $G(\theta, \phi) = \delta(\theta)\delta(\phi)$, so that that spectrum peaks at

$$f_z = f_T \left(1 - 2\frac{w}{c} \right).$$

More generally, it can be seen in (16) that there is a term in $\sin^2\phi$, so that there is a contribution from the traverse width of the beam in spite of G being even in ϕ . The influence of this term in v is to give a broader spectral peak but not to change the peak position substantially, so it will be ignored in the following. Also, in general, the effect of the $\sin\theta$ weighting on u is to bias the spectral peak to the equivalent of a larger effective θ_0 . There is, therefore, a small change in the effective tilt

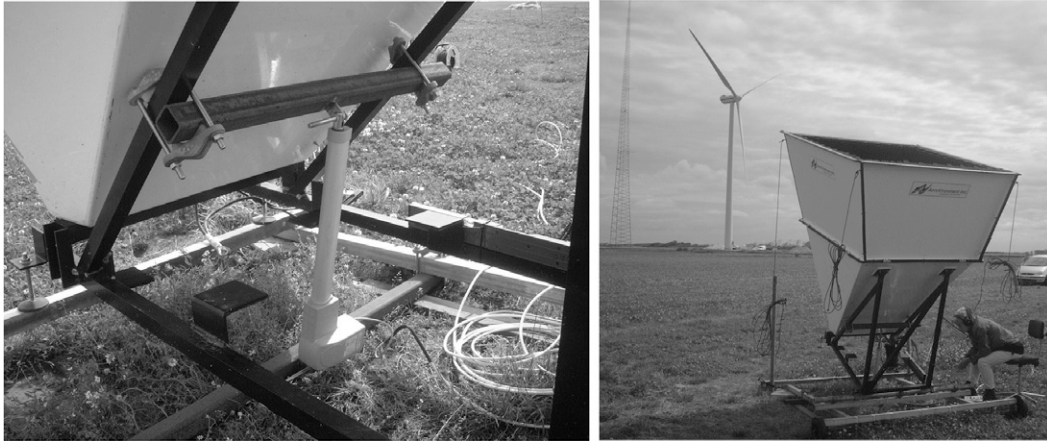


FIG. 2. (left) Mounting frame and linear actuator with digital level and (right) measurements being taken.

angle, as expected. However, this does not change the methodology of the new calibration concept when the effective tilt angle is unknown anyway.

5. Error analysis

Writing σ_V for the uncertainty in wind speed V , (13) gives

$$\sigma_{\theta_1}^2 \approx \left(\frac{\tan\theta_1}{\tan\Delta\theta} \right)^2 \left[\sigma_{\Delta\theta}^2 + \left(\frac{\sigma_V \sin\theta_1}{V} \right)^2 \right].$$

To obtain a calibration accuracy of 1%, we need $\sigma_\theta \approx 0.2^\circ \approx 4 \times 10^{-3}$ radian. For $\theta_1 = \Delta\theta = 15^\circ$, and without any peak detection error, $\Delta\theta$ also needs to be measured to 0.2° . This is achievable with a linear actuator and a digital inclinometer. The accuracy of 10-min averaged sodar spectral peak estimation is typically $\sigma_V = 0.2 \text{ m s}^{-1}$, so the term in σ_V is typically a factor of 10 larger than the $\sigma_{\Delta\theta}$ term. What this means is that around 10 trials of 10-min duration must be conducted in order to reduce the typical errors from peak detection to an acceptable level.

An alternative is to recast (13) in the form

$$Y = aX,$$

where

$$Y = \frac{V_{r3}^2 - 2V_{r3} V_{r3}^* \cos\Delta\theta + V_{r3}^{*2}}{V_{r1} V_{r3}^* - V_{r1}^* V_{r3}}$$

and $X = \sin\Delta\theta$. The slope of the least squares line through the origin is $a = 1/\sin\theta_1$.

A disadvantage of this method is that the radial velocity components may not be made available to the user by the sodar manufacturer. They then need to be calculated

based on the beam zenith angle assumed by the manufacturer, or the zenith angle is calculated from the antenna parameters. An alternative, and a much simpler procedure, is to assume that, in comparison with u and v , w is negligible, so

$$\frac{u^*}{u} - \cos\Delta\theta = \left(\frac{1}{\tan\theta_1} \right) \sin\Delta\theta,$$

which means that θ_1 can be estimated from the slope of the straight-line fit through the origin, via

$$\tan\theta_1 = \frac{\sum_{n=1}^N (\sin\Delta\theta_n)^2}{\sum_{n=1}^N \left(\frac{u_n^*}{u_n} - \cos\Delta\theta_n \right) \sin\Delta\theta_n}.$$

In this case

$$\sigma_{\theta_1}^2 \approx \frac{2}{\sum_{n=1}^N \sin^2\Delta\theta_n} \left(\frac{\tan^2\theta_1}{1 + \tan^2\theta_1} \right)^2 \left(\frac{\sigma_V}{V} \right)^2,$$

where N measurements are taken at $\Delta\theta_n, n = 1, 2, \dots, N$. For $\theta_1 = 15^\circ$ and $\sigma_V/V = 0.04$, three cycles of $\Delta\theta = 15^\circ$ and 38° should give $\sigma_\theta < 0.2^\circ$.

6. Field measurements

Field measurements on very flat land in western Denmark have been completed on an Atmospheric Systems Corporation (ASC) 4000 sodar mounted on a frame, which is then tilted using a 12-V-powered linear actuator, as shown in Fig. 2. The operator used a reversing

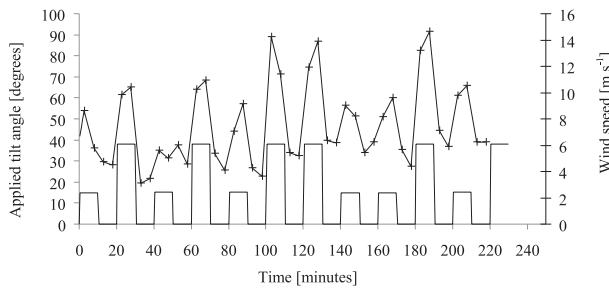


FIG. 3. Wind speed (crosses) and tilt angle (solid line) plotted vs time.

switch to raise and lower the tilting platform in synchronism with the sodar averaging time, so that one undisturbed averaging period was followed by an averaging period in which the actuator was moved. Tilt angle $\Delta\theta$ and 90-m wind speed versus time are shown in Fig. 3. The correlation between retrieved wind speed and tilt angle is strong. This is expected from (7), which shows that V_{r1}^* is essentially linear in $\Delta\theta$.

7. Data analysis

Wind vector components were recorded at 10-m-height intervals from 30 to 130 m. The beam zenith angle θ_1 was estimated from the least squares slope of the line through the origin for both the $w = 0$ case and the full solution case. Variances of the Y values corresponding to each of the two tilt angles were used as least squares weights, since it was expected that the radial wind variability would increase as the sodar was tilted further. Figure 4 shows estimated θ_1 values at each height for the two cases. The lowest height gives outlier values of angle, consistent with some clutter contamination from beam sidelobes when the beam is tilted. The estimated angle at the upper height (130 m) also appears to give an outlier, especially for the $w = 0$ case, consistent with the

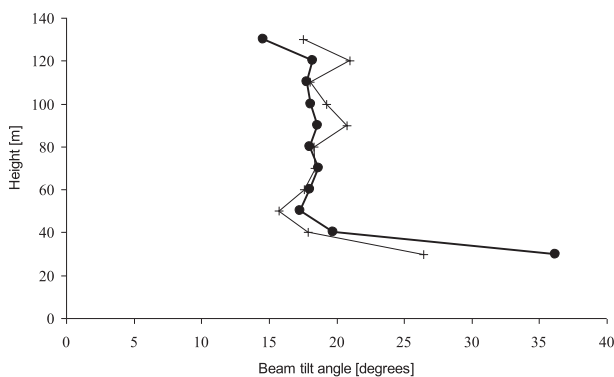


FIG. 4. Estimated beam zenith angles θ_1 from the $w = 0$ case (filled circles) and the unconstrained w case (plus signs).

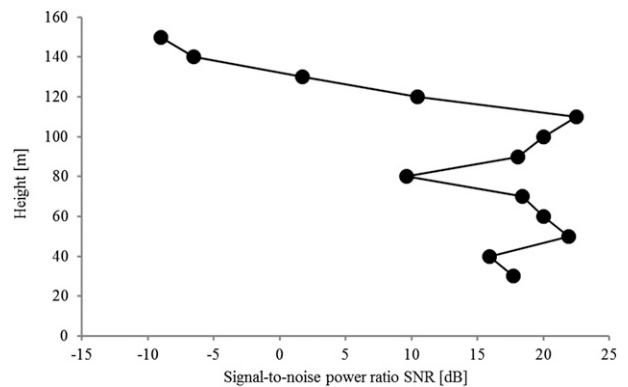


FIG. 5. Mean SNR for the w beam, as a function of height.

signal-to-noise ratio (SNR) for sodar signals decreasing rapidly above 120 m (see Fig. 5).

The expected value of θ_1 can be calculated from the phased-array geometry for this sodar. An incremental phase shift of $\pi/2$ is used to change beam zenith angles. The beam maximum will therefore be at a zenith angle of $\theta_1 = \sin^{-1}(\lambda/4d)$, where λ is the wavelength and d is the array element spacing. In the case of this sodar, the transmitted frequency was 4500 Hz, and the speakers have a diameter of 0.085 m but are used in diagonal rows of spacing $d = 0.085/2^{1/2} = 0.06$ m. Taking into account the mean air temperature at sodar height during the experiment, $\theta_1 = 18.32^\circ$. This compares with the estimated zenith angle from the two cases given in Table 1.

8. Conclusions

Since Doppler measurement is inherently calculable, the main source of systematic calibration errors for sodars is uncertainty regarding the effective beam pointing angle.

A new method for beam geometry calibration of sodars is described. The method makes no assumptions about the sodar operation and its hardware and software, other than the assumption that only one beam is transmitted at a time and that the flow is horizontally homogeneous. Regardless of the complexity of the actual beam shape, the *effective* beam tilt angle is accurately estimated: this is the angle that must be used in estimations of velocity components. In a very simple

TABLE 1. Comparison between estimated beam zenith angles ($^\circ$) and the calculated zenith angle ($^\circ$).

	Mean θ_1	$\sigma_{\text{mean } \theta}$	Estimated – calculated θ_1
Calculated θ_1	18.32	—	—
θ_1 estimated with $w = 0$	18.27	0.23	-0.05
θ_1 estimated with $w \neq 0$	18.55	0.54	0.23

experiment, the effective beam zenith angle has been found to within around 0.2° , which is as good as is required in the most stringent sodar calibration procedures. It has been found, even for such a short data run, that the estimated angle is very close to that calculated from the sodar array geometry.

Atmospheric refraction effects are not significant here. For example, with a beam zenith angle of 45° , an adiabatic lapse rate, and a height range of 100 m, the change in propagation angle is only around 0.1° . The main limitation evident at this stage is the requirement for horizontally homogeneous flow, since the regression methods use both a tilted beam and a vertical beam. Note that this is also a fundamental limiting assumption in the normal *operation* of ground-based wind lidars and sodars. However, since horizontal homogeneity of the flow is assumed, this method should only be applied over flat homogeneous terrain, and not when strong vertical gradients might be expected. The vertical gradient restriction is because there is also the assumption that the wind at a particular radial distance for the artificially tilted beam is the same as the wind at the same range without artificial tilting. For example, with the 40° artificial tilt applied here, this means that the wind at 100-m height should be similar to the wind at 80-m height. Given the extended vertical sampling volume of the sodar, this assumption will not normally cause significant errors. Note that both sodars and lidars are used with the assumption (generally not stated) that the sampling in the vertical, via “range gating,” is adequate to describe the vertical structure of the wind, and that spatial aliasing is not occurring.

There are a number of reasons why the method described above is of practical importance. These include the fact that there will be a bias in measured Doppler shift compared to that calculated from simple beam geometry because, for a beam symmetric around the central tilted direction, the angles between wind vector and portions of the beam are not symmetrical about the central direction. Furthermore, there can be bias arising from clipping of the beam by acoustic baffles surrounding the instrument, and these effects are generally difficult to estimate or measure in other ways. Similarly, it is challenging to calculate with confidence the beam shape of a sodar based on small parabolic dish reflectors, such as the AQSystem AQ500. Even for a sodar based on a phased array of transducers, the beam shape details depend on the relative gains of the transducer elements, which may not be known with confidence, especially after the sodar has been deployed in the field for some time.

Acknowledgments. The authors are grateful for support from Michael Courtney, Torben Mikkelsen, and the Høvsøre staff at Risø/DTU, and to Christine Bradley for field observations.

REFERENCES

- Bradley, S. G., 2008: *Atmospheric Acoustic Remote Sensing: Principles and Applications*. CRC Press/Taylor and Francis Group, 271 pp.
- , I. Antoniou, S. von Hünerbein, D. Kindler, M. de Noord, and H. E. Jørgensen, 2005: SODAR calibration for wind energy applications. Final Reporting on WP3, EU WISE Project NNE5-2001-297, University of Salford, 70 pp.